5th Australasian Congress on Applied Mechanics, ACAM 2007
10-12 December 2007, Brisbane, Australia

Micro-Indentation of Metal Matrix Composites: A 3D Finite Element Analysis

A. Pramanik, J. A. Arsecularatne and L. C. Zhang

School of Aerospace, Mechanical and Mechatronic Engineering, The University of Sydney, NSW-2006, Australia

Abstract: This paper investigates the inhomogeneous behavior of MMCs subjected to micro-indentation by a spherical indenter using 3D finite element analysis. This includes the effects on hardness of volume percentage of reinforced particles and indenter-to-particle diameter-ratio. It was found that the increase of volume percentage of reinforced particles and indenter-to-particle diameter-ratio increases the resistance to deformation of an MMC. The hardness varies in a complex way with the changes of load, volume percentage of particles and indenter-to-particle diameter-ratio.

Keywords: Metal Matrix Composites, Micro-indentation, Hardness, Finite Element Analysis.

1 Introduction

Metal matrix composites (MMCs) have a high strength to weight ratio and wear resistance, and are increasingly used in automotive and aerospace structures [1-2]. While the reinforcement induces superior tribological and strength properties, the reinforcement particles also bring about difficulties in characterization [3]. Micro-indentation is an effective and simple means to understand the performance and deformation of MMCs [4]. However, most investigations on the properties of MMCs have been experimental [5-7] and do not provide detailed analysis of the deformation during loading/unloading for different particle-matrix-indenter arrangements. The present study will investigate the deformation behaviour of MMCs due to micro-indentation and its influence on hardness and strain development using 3D finite element analysis.

2 Modelling

To achieve a deeper understanding of the effects of the reinforcement particles, this paper will use a three dimensional finite element model to investigate the influence of locations of indentation relative to particles (LIRP). Two types of indentations will be carried out: (1) indenting exactly above a particle (IAP) (Fig. 1(a)), and (2) indenting at the middle of four particles (IMP) (Fig. 1(b)).

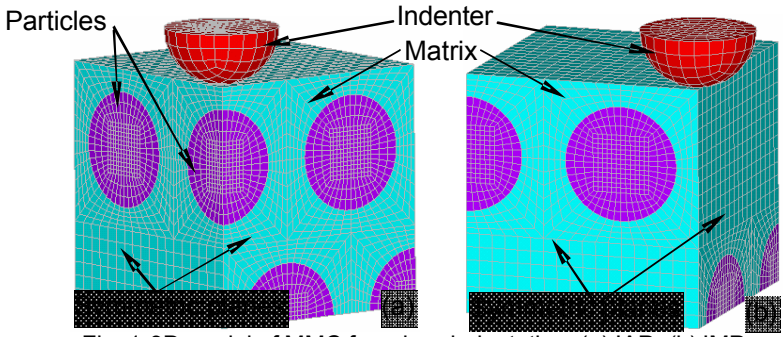

Fig. 1 3D model of MMC for micro-indentation: (a) IAP, (b) IMP

Symmetric boundary conditions were applied on the MMC to make the model size manageable (Fig. 1) [4]. Particles were assumed to be uniformly distributed and perfectly bonded with the matrix. The indentation process was considered to be quasi-static. The workpiece was fully fixed on its bottom surface to eliminate rigid body motion. The length and height of the workpiece were selected to be sufficiently large to avoid boundary effects. Particle fracture was not considered. The FEA was performed using ANSYS/LS-DYNA with the maximum element size being 2.08 μm. The simulation had been repeated with mesh refinement which brought about negligible differences in results.

The MMC work material was a 6061 aluminium alloy reinforced with spherical silicon carbide particles. The reinforcements were treated as isotropic perfectly elastic with Young's modulus = 400 GPa and Poisson's ratio = 0.17. The 6061 Al matrix followed a temperature-independent bilinear kinematic hardening material model and its associated flow rule. The corresponding stress-strain curve given in

Fig. 2 was based on the data in [5]. The properties of the matrix were: Young's modulus E = 71.6 GPa, Poisson's ratio v = 0.33, yield strength = 125 MPa, tangent modulus = 1.48 GPa. The diamond indenter was assumed to be linear elastic with E = 1147 GPa and v = 0.070. The average friction coefficient of μ = 0.6 [1] was used in the present analysis.

To understand the response of MMCs in relation to LIRP, size ratio of indenter to particle (SRIP), indentation load, volume percentage of particles, and properties of matrix and particles, this study used the following conditions: volume percentage of particles = 10, 20 & 30%; diameter of the indenter = 16.2, 18, 21.6 & 25.2 μm; control volume = 37.5 μm x 37.5 μm x 37.5 μm.

3 Results and discussions

3.1 Force-displacement behavior

In the force-displacement curves (Fig. 3) the displacement represents elastic plus plastic displacement of the indenter. These curves are related to the elastic modulus and hardness of the work material, but compared with a monolithic material it is more difficult to interpret them in terms of hardness, tensile strength, ultimate strength and modulus of elasticity [8]. For example, the gradient of the force-displacement curves (Fig. 3) varies with indentation load, LIRP, SRIP, etc.

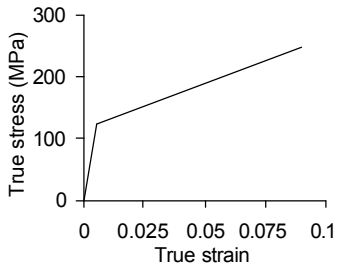

Fig. 2. The stress versus strain curve for 6061 aluminium matrix

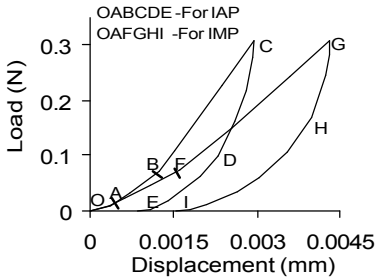

Fig. 3. Load displacement curves for different LIRP (SRIP = 1 and particle volume % = 20)

Fig. 3 shows that the load-displacement curves for cases IAP and IMP, and the former shows a higher stiffness. There are two obvious changes along the load-displacement curves, at points A and B for IAP, and A and F for IMP. This phenomenon was experimentally observed by Mussert et al. [8], and it was attributed to the presence of particles. During unloading, curves for IAP and IMP followed similar trend of spring back though the gradient of IAP curve is higher than that of IMP curve. At a given applied maximum load the residual plastic deformation on unloading is smaller for IAP than for IMP.

Initially the resistance to matrix flow by the particles is negligible for both cases (part OA along the curves). After point A, particles restrict matrix flow and matrix between indenter and particles experiences high deformation. This results in a trend change of load-displacement curve. For the IMP, the restriction to matrix flow is less and indentation displacement is higher than those for IAP at the same indentation load. Hence, AB shows a higher stiffness than AF. At B and F, secondary indentation starts to take place, i.e. the reinforcement particle is being pushed down in the matrix and starts to act as an 'indenter' inside. Consequently, the force-displacement curves indicate distinct increase of gradient (hence stiffness) which is consistent with experimental results in [8].

Higher load bearing capacity of reinforcing particles reduces the deformation of the MMC under loading [3, 6]. The total deformation of the MMC for IAP is lower than that of IMP at a given indentation load because in this case particle which carries higher load is located closer to the indenter. After unloading, the elastic particle will return to its undeformed form but plastic matrix will remain deformed. Hence, higher plastic deformation is noted during IMP. These will be further discussed below.

3.1.1 Effect of volume percentage of particles

Figs. 4(a) & (b) present the load-displacement responses during loading and unloading for different volume percentages of reinforcements for both IAP and IMP. At the start of the indentations, all the curves show almost the same trend but with further loading, they indicate varying stiffness. Higher the volume percentage of reinforcements, higher is the stiffness increment. After unloading, lower plastic deformation is noted for the MMC with a higher volume percentage of reinforcement.

A loading curve with higher stiffness indicates higher resistance to deformation. Increase of volume percentage of particle means decrease of volume percentage of matrix material (MM) and an increase

of particle number (for a constant particle size). Hence, an increased number of particles will take part in resisting matrix flow and carrying loads in the composite. Thus it is clear that, with the increase of volume percentage of reinforcements, resistance to deformation increases, i.e., the loading curves show greater stiffness. The above mechanism will make an MMC with a higher volume percentage of reinforcements show lower plastic deformation. These are also affected by LIRP due to variation of distance between indenter and particle. It seems that the ceramic particles increase the Young's modulus and decrease plasticity of MMCs.

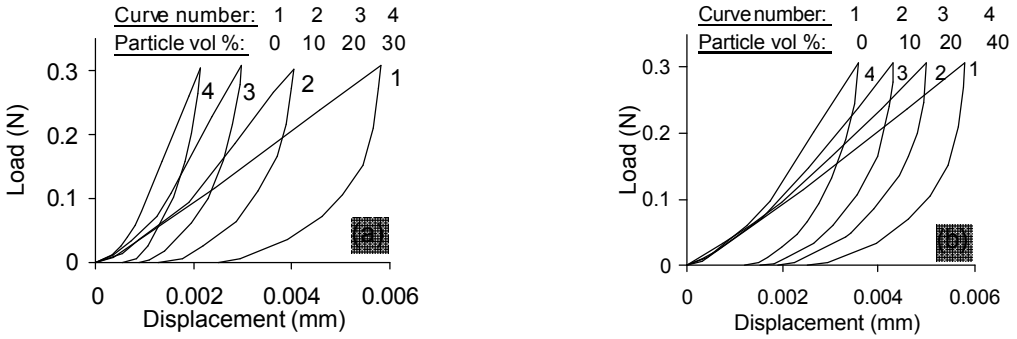

Fig. 4 Effects of reinforced particle vol% on load-displacement curves (SRIP = 1): (a) IAP, (b) IMP

3.1.2. Effect of the SRIP

The effects of particle size as well as indenter size can be accounted by considering the size ratio of indenter to particle. Figs. 5(a) & (b) show the effects of this ratio on the load-displacement curves for the two types of LIRP. As with the effects of volume percentage of reinforcements discussed earlier, at the start of indentation, the gradients of load-displacement curves are similar for each case. But with the increase in indentation load, the curves start to deviate at different stages of loading. A load-displacement curve corresponding to a higher SRIP shows higher stiffness (Figs. 5(a) and (b)). Once again the load-displacement curves for the IAP case show higher stiffness compared to those for IMP case. Thus the resistance of an MMC to deformation increases with the increase of SRIP. For the ranges of forces and displacements investigated, after unloading, almost constant plastic deformation is noted for all the SRIP considered (Figs. 5(a) & (b)) but plastic deformation of MMC is higher for IMP than that of IAP. This indicates that, for the tested range of loads, etc., the size of indenter has negligible influence on plastic deformation (depth of indentation) of MMCs.

With the increase of indenter diameter, a larger contact area and hence a higher resistance due to reinforced particles occurs at a given indentation load. Therefore, the total deformation of an MMC decreases with the increase of SRIP (Fig. 5). Consequently the load-displacement curve shows higher stiffness at higher SRIP.

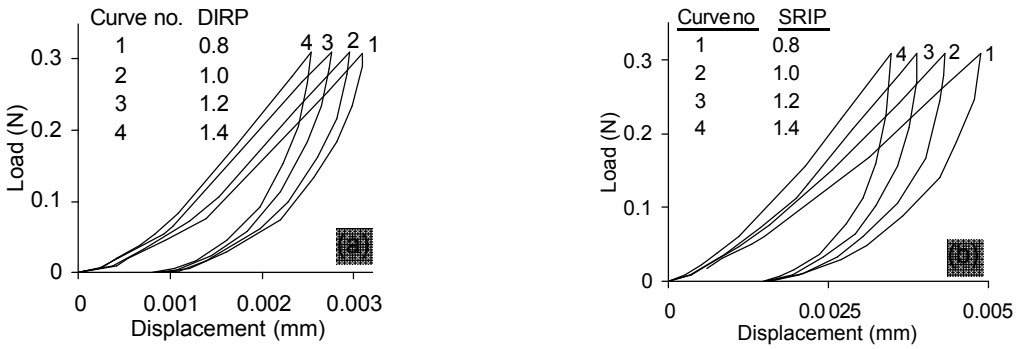

Fig. 5. Effects of SRIP on load-displacement curves (particle volume % = 20) (a) IAP, (b) IMP

3.2 Hardness

The hardness was determined from Hardness = P/(πDt), where *P* is the applied load, *D* is the diameter of indenter and *t* is the depth of the indentation after complete unloading.

3.2.1 Effects of indentation load on hardness

Hardness of a material obtained by indentation is a measure of its resistance to plastic deformation. Micro-hardness of an MMC, compared to a monolithic material may show a greater dependence on indentation load because of its inhomogeneous deformation behavior due to the presence of

reinforcement particles. The indentation loads selected correspond to points A, B, C, F and G on the load-displacement curves in Fig. 3. These points were selected to investigate the effect of gradient changes of load-displacement curve on the hardness of an MMC. Some high loads beyond points C and G were also considered to observe hardness variation over a wider range of loads. Indentations were performed with loads at corresponding points and then it was unloaded completely to obtain corresponding *D* and *t* values. The hardness values corresponding to these loads were then calculated. The variation of hardness (Fig. 6) can be explained as follows.

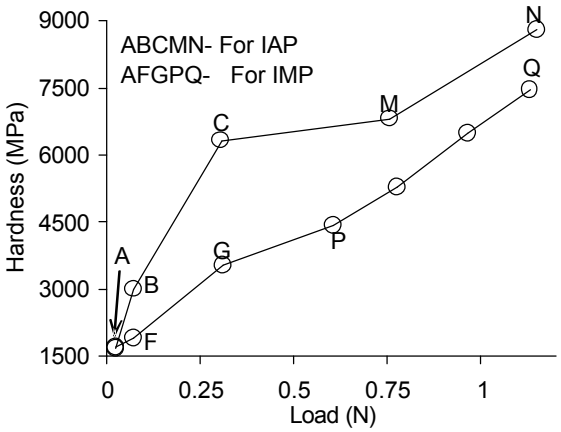

Fig. 6 Effects of indentation load on hardness of MMC (SRIP = 1 and particle volume % = 20)

For indentation with a very low load, the effect of LIRP is small (point A in Fig. 6). With the increase of indentation load, particles restrict the matrix flow and the hardness of the MMC continues to increase due to higher resistance to plastic deformation of MM. For IAP, the resistance to plastic deformation is much higher than that for IMP case due to the greater resistance by the particles on the matrix flow in the former (Sec. 3.1). Hence the rate of increase of hardness with increase of indentation load is higher for the IAP case, i.e., gradient of AB is higher than that of AF. At points B and F, secondary indentation by particles near the indenter takes place, which causes a further increase of hardness. The increase of hardness is much higher for IAP case (BC) than that of IMP (FG). Then the matrix below the particle (secondary indenter) starts to deform significantly and secondary indentation occurs with the increase of loading. The secondary indentation and associated additional restriction on matrix flow further increases the hardness (CM and GP in Fig. 6) depending on the MM properties, particle concentration, size and shape [7]. After points M and P, particles around the secondary indenter apply significant constraint to matrix flow. At this stage primary and secondary particles (those below the primary particle) come closer. This further restricts the matrix flow, resulting in an increase in the local hardness [9]. Therefore, hardness continues to increase with loading. Since the reinforcement particles are much stiffer than the matrix, they carry a significant fraction of load during indentation.

Leggoe et al. [10] experimentally showed that the presence of reinforcement particles restricts matrix flow in an MMC resulting in a higher hardness during indentation. This was also noted in the present investigation as described above. The higher the indentation force/displacement, the higher is the particle concentration underneath the indentation [9]. The increase of hardness with the increase of load in the stabilizing stage for a particle reinforced MMC can be attributed to the localized increase in particle concentration directly underneath the indenter during a hardness test [6].

3.2.2 Effects of volume percentage & SRIP

To investigate the effect of reinforcement volume percentage and SRIP on hardness, a constant indentation load, 0.308 N, was used on the basis of sufficient deformation. Fig. 7 presents the effect of reinforcement volume percentage. It is clear that hardness of an MMC increases with the increase of volume percentage of reinforcement for both cases. However, due to the higher rate of increase, the hardness is much higher for IAP. It seems that further addition of reinforcement particles top ups the hardness over that of IMP. It was noted (Sec. 3.1.1) that an MMC with a higher percentage of reinforcements has higher resistance to deformation and lower plastic deformation (Figs. 4(a) & (b)). Hence, MMCs with higher percentages of reinforcements show higher hardness.

Fig. 8 shows the influence of SRIP. With the increase of SRIP, hardness is found to decrease. An interesting feature is that the rate of decrease with SRIP is similar for the two LIRP cases. As discussed in Sec. 3.1.2, during indentation, with the increase of SRIP, MMCs show little increase of

total deformation during loading but no significant variation in plastic deformation (depth) after unloading. Since, with the increase of SRIP, plastic deformation of an MMC does not vary but the diameter of indenter increases and the hardness decreases.

3.3 Development of strain fields

The contours of von Mises total strain at different points on load-hardness curves (Fig. 6) are presented in Fig. 9. These explain the deformation mechanism of an MMC and hardness changes over the range of loading considered. Strains developed in the indenter and reinforced particles during indentation process are negligible compared to those of MM because of high modulus of elasticity of the indenter and particles. Hence, only the strain development in the MM is considered here. This will also include details at the particle-matrix and indenter-matrix interfaces.

3.3.1 Indentation above a particle

Fig. 9 depicts the variation of the total von Mises strain in the MMC for IAP. At the start of loading (not shown in Fig. 9), the maximum strain is near the contact interface. The strain field did not extend to the particle-matrix interface and the effect of particle is small. This stage corresponds to point A in Figs. 3 & 6. With further loading, the strain field expands and reaches the particle-matrix interface (B in Figs. 3 & 6, not shown in Fig.9). At this stage the maximum strain zone approaches the particle and the strain is in excess of 0.84. As the loading continues, significant matrix deformation under the particle starts, which causes secondary indentation in the matrix by the reinforced particle (Fig. 9 (a)). The resulting deformation continues until the effect of secondary particle becomes significant. Fig. 9(b) represents the strain state at point M in Fig. 6 and the maximum strain here is in excess of 2.2. During tertiary deformation (not shown in Figure 9) the particle constrains the matrix flow.

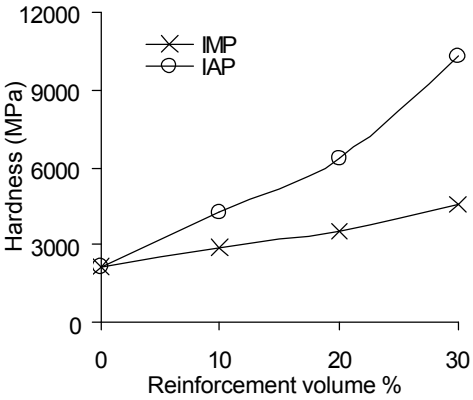

Fig. 7. Effect of reinforcement volume percentage on hardness of MMC (SRIP = 1, particle volume % = 20 and indentation load = 0.308 N)

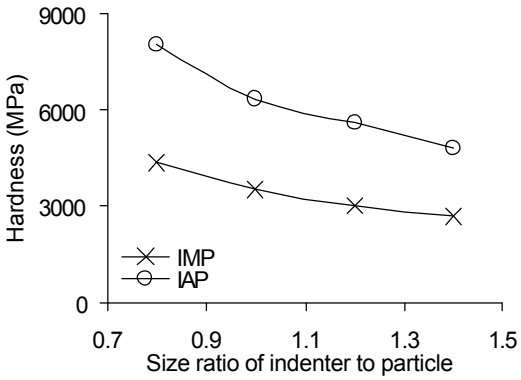

Fig. 8. Effect of SRIP on hardness of MMC (particle volume % = 20 and indentation load = 0.308 N)

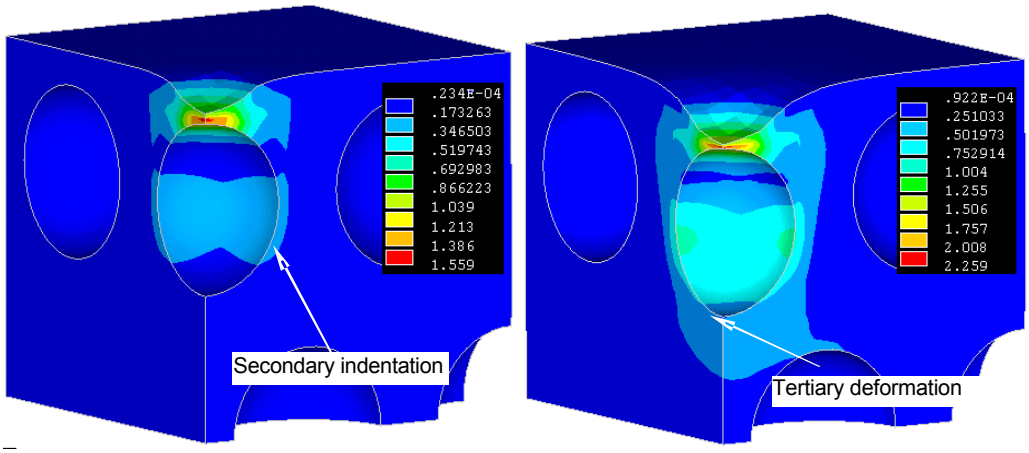

(a) At point C in Fig. 6 (c) At point M in Fig. 6

Fig. 9 The total on von Mises strain in the matrix for IAP (SRIP = 1 and particle volume % = 20)

3.3.2 Indentation between particles

For IMP, the development of the strain field is qualitatively similar to that described in Sec. 3.3.1; but the maximum strains at the corresponding points are considerably lower. It is interesting to note that the point with the maximum strain initially appears near the indenter, but with continued loading it moves towards the particle and eventually reaches the particle-matrix interface. Secondary indentation then starts and the strain state corresponds to that at point F. The same phenomenon was noted for the IAP.

It can be concluded that initial yielding of the matrix occurs near the indentation interface and then extends to the particle-matrix interface(s) through the matrix. The presence of particles dramatically affects the plastic field and causes extreme inhomogeneous deformation and flow of matrix in the MMC. Thus localized deformation of the MMC can be expected after indentation. The amount of deformation of the MMC depends on the LIRP. These are in agreement with the experimental observations [11]. Additionally, and as with a monolithic material subjected to indentation, yielding occurs first at a small distance beneath the indentation interface (Fig. 9 (a)).

4 Conclusions

Due to the presence of reinforcements, MMCs behave very differently compared to monolithic metals during deformation. The present investigation has shown that:

(i) The hard ceramic particles increase the MMC's ability to resist deformation which is highly dependant on the location of indentation relative to particles, volume percentage of particles, size ratio of indenter to particle and applied load. Consequently, these parameters affect hardness of MMCs.

(ii) The mechanisms responsible for the anisotropy of MMCs are: varied restriction to matrix flow by particles and non-uniform work hardening of MM depending on the combination of above mentioned parameters.

(iii) It is inappropriate to use the conventional micro-hardness to measure the properties of MMCs when the indentation load is low.

Acknowledgements

The authors wish to thank the ARC for financial assistance. AP is under IPRS and IPA scholarships.

References

[1] A. Pramanik, L. C. Zhang, J. A. Arsecularatne, Int. J of Machine Tools and Manufacture 46(2006) 1795-1803.

[2] Z. F. Zhang, L. C. Zhang, and Y.W. Mai, Journal of Materials Science, 30(23) (1995) 5999-6004.

[3] A. Pramanik, L. C. Zhang, J. A. Arsecularatne, Int. J of Machine Tools and Manuf, 47 (2007) 1497-1506.

[4] A. Pramanik, L. C. Zhang, J. A. Arsecularatne, Key Engineering Materials, 340-341 (2007) 563-570.

[5] S. G. Long, Y. C. Zhou, Composites Science and Technology, 65 (2005) 1391–1400.

[6] Y. L. Shen, J. J. Williams, G. Piotrowski, N. Chawla and Y. L. Guo, Acta mater. 49 (2001) 321-3229.

[7] J. W. Leggoe, Journal of Materials Research, 19 (8) (2004) 2437-2447.

[8] K. M. Mussert, W. P. Vellinga, A. Bakker, S. Van Der Zwaag, Jl of materials science, 37 (2002) 789-794.

[9] R. Pereyra, Y. -L. Shen, Material Characterization 53 (2004) 373-380.

[10] J. W. Leggoe, X. Z. Hu, M. V. Swain, M. B. Bush, Scripta Metallurgica *et* Materialia, 31(5) (1994) 577-5825.

[11] K. Unterweger, O. Kolednik, Material Research and Advanced Techniques, 96 (9) (2005) 1063-1068.